Available online at www.sciencedirect.com
ScienceDirect
Icarus ••• (••••) •••–•••
ICARUS
www.elsevier.com/locate/icarus

Impacts as sources of the exosphere on Mercury

Alexey A. Berezhnoy [a,b,*], Boris A. Klumov [c]

[a] *Sternberg Astronomical Institute, Moscow State University, Universitetskij pr., 13, 119991 Moscow, Russia*
[b] *Rutgers University, Department of Chemistry and Chemical Biology, 610 Taylor Road, Piscataway, NJ 08854-8087, USA*
[c] *Max-Planck-Institut für Extraterrestrische Physik, D-85740 Garching, Germany*

Received 29 August 2007; revised 13 January 2008

Abstract

Chemical processes associated with meteoroid bombardment of Mercury are considered. Meteoroid impacts lead to production of metal atoms as well as metal oxides and hydroxides in the planetary exosphere. By using quenching theory, the abundances of the main Na-, K-, Ca-, Fe-, Al-, Mg-, Si-, and Ti-containing species delivered to the exosphere during meteoroid impacts were estimated. Based on a correlation between the solar photo rates and the molecular constants of atmospheric diatomic molecules, photolysis lifetimes of metal oxides and SiO are estimated. Meteoroid impacts lead to the formation of hot metal atoms (0.2–0.4 eV) produced directly during impacts and of very hot metal atoms (1–2 eV) produced by the subsequent photolysis of oxides and hydroxides in the exosphere of Mercury. The concentrations of impact-produced atoms of the main elements in the exosphere are estimated relative to the observed concentrations of Ca, assumed to be produced mostly by ion sputtering. Condensation of dust grains can significantly reduce the concentrations of impact-produced atoms in the exosphere. Na, K, and Fe atoms are delivered to the exosphere directly by impacts while Ca, Al, Mg, Si, and Ti atoms are produced by the photolysis of their oxides and hydroxides. The chemistry of volatile elements such as H, S, C, and N during meteoroid bombardment is also considered. Our conclusions about the temperature and the concentrations of impact-produced atoms in the exosphere of Mercury may be checked by the Messenger spacecraft in the near future and by BepiColombo spacecraft some years later.

Keywords: Impact processes; Mercury, atmosphere; Photochemistry

1. Introduction

Mercury has a tenuous exosphere; the content of atoms in this exosphere is controlled by the dynamical balance between different sinks and sources. The concentrations and temperature of Na and K in the exosphere can be explained by photon stimulated and thermal desorption (Yakshinskiy and Madey, 2000). The release of ions, atoms, and molecules from the surface occurs by chemical sputtering (Potter, 1995) and also by solar wind sputtering (Potter and Morgan, 1990). Sudden increases of the Na emission flux on Mercury may be explained by meteoroid impacts (Leblanc et al., 2006). Meteoroid impacts are considered to be one of the main sources of calcium in the exosphere of Mercury (Killen et al., 2005). Killen and co-workers proposed that calcium is delivered in the form of calcium oxide. Other sources of exospheric Ca discussed in the literature include ion sputtering (Killen et al., 2005) and solar wind (Koehn and Sprague, 2007). Meteoroid bombardment is a more important source for the night side of the planet because ion sputtering produces atoms in the exosphere only on the day side.

Study of the composition of the impact-produced exosphere of Mercury is also useful for estimating the elemental composition of the surface of the planet, which is still poorly known. For a detailed study of the exosphere of Mercury, optical and ultraviolet spectrometers on board the NASA Messenger (McClintock and Lankton, 2007) and ESA-JAXA BepiColombo (Yamakawa et al., 2004) spacecraft will be used. These missions have significantly revived interest in the nearest planet to the Sun. The monitoring of the concentrations of impact-produced atoms in the exosphere of Mercury by these spacecrafts can be used to study of meteor showers on Mercury

* Corresponding author at: Sternberg Astronomical Institute, Moscow State University, Universitetskij pr., 13, 119991 Moscow, Russia. Fax: +7 495 932 8841.
E-mail address: aaberezh@yandex.ru (A.A. Berezhnoy).

0019-1035/$ – see front matter
doi:10.1016/j.icarus.2008.01.005

Please cite this article in press as: A.A. Berezhnoy, B.A. Klumov, Impacts as sources of the exosphere on Mercury, Icarus (2008), doi:10.1016/j.icarus.2008.01.005

and to estimating the mass flux of meteoroids to the planetary surface.

The main goal of this paper is to predict the abundances and the temperatures of impact-produced atoms of the main elements in the exosphere of Mercury. Our results can be checked by NASA Messenger mission in the near future. Recently, Mangano et al. (2007) estimated the probability that instruments aboard BepiColombo and/or Messenger would detect impact-produced metal atoms. Mangano and co-workers assumed that meteoroid impacts produce only metal atoms and not molecular species in the exosphere. A possible indirect effect on their results, the influence of molecular photolysis on the temperature of metal atoms, was not taken into account. More generally, the chemistry of impact-induced clouds (or fireballs) produced by meteoroid impacts has not yet been considered in detail. We investigate this problem by modeling theoretically the concentrations of species containing Na, K, Ca, Fe, Al, Si, Mg, Ti, O, H, S, C, and N as an impact-induced cloud evolves. For this purpose we adapt the model of Berezhnoi and Klumov (1998), which was developed to treat larger impacts on the Moon, for the case of smaller impactors. In the original treatment of Berezhnoi and Klumov (1998), only the behavior of volatile elements during impact processes on the Moon was considered. We extended this work to study refractory elements as well.

The paper is organized as follows. First, we estimate the initial parameters of the impact-induced vapor cloud expansion and its elemental composition and use quenching theory to model the physical and chemical evolution of the fireball. Limitations of the quenching theory are also discussed. Second, we estimate the photolysis lifetimes of metal monoxides and SiO based on a known correlation between solar photolysis rates and molecular constants for known atmospheric diatomic molecules. We find that photolysis lifetimes are shorter than ballistic flight times for major diatomic species. Thus, the photolysis of molecular species increases the content of atoms in the exosphere of Mercury. Then we estimate the temperature and the concentration of impact-produced atoms of major elements both with and without considering condensation and compare our predictions with available observational data. It is shown that ionization of neutral atoms decreases the content of atoms in the exosphere by a few percent at most.

2. Physics and chemistry of meteoroid impacts

2.1. Formation and cooling of the fireball

Collisions of meteoroids with Mercury with typical impact speeds of 10–80 km/s lead to vaporization of the impactor, vaporization, melting, and fragmentation of the regolith, and then to the ejection of multiphase impactor matter and planetary soil. While impact-induced cloud consists of a mixture of vapor, liquid, and solid we consider only vapor because only gas-phase compounds are delivered to the exosphere by impacts. We first estimate the initial temperature and pressure in the fireball. The initial temperature of the impact-induced cloud T_0 can be estimated as

$$T_0 = \eta M_\mathrm{i} V_\mathrm{i}^2/(2C_\mathrm{v}M_\mathrm{v}), \tag{1}$$

where η is the part of kinetic energy of the impactor released for heating of the impact-produced vapor, M_i, V_i are the mass and velocity of the impactor, respectively, M_v is the mass of the impact-produced vapor, $C_\mathrm{v} \approx 3000\,\mathrm{J\,kg^{-1}\,K^{-1}}$ is the heat capacity of the gas at constant volume, a value typical for the considered case.

Small meteoroids with radii in the range 10^{-8}–10^{-2} m typically strike Mercury with velocities between 10 and 40 km/s, but 1–10 cm meteoroids collide with Mercury with velocities between 20 and 70 km/s (Cintala, 1992). The impactor–target mass ratio in the impact-induced cloud depends on impact velocity. We use the approach of Ahrens and O'Keefe (1987) for estimating the mass of the impact-produced vapor for the case of vertical impacts

$$M_\mathrm{v} \approx M_\mathrm{i}\left(2\left[4(Q_\mathrm{v}/\nu)^{0.5}/V_\mathrm{i}\right]^{\nu-2} - 1\right). \tag{2}$$

Formula (2) was obtained by Ahrens and O'Keefe (1987) from numerical modeling of impact processes. The parameter ν was taken to be 0.33, a value typical for continuous media. The evaporation heat of the target, Q_v, was taken to be 1.3 MJ/kg, a value typical for silicates. Using these assumptions, we find that the mass of vapor in impact-induced cloud may reach 10 impactor masses at 20 km/s and 60 impactor masses at 60 km/s.

From formulas (1) and (2) and assuming $\eta = 0.3$ we find $T_0 = 10{,}000$ K for 30 km/s impacts. The value of T_0 increases slightly with increasing impact velocity as $(V_\mathrm{i})^\nu$.

The initial temperature and pressure can be determined by numerical modeling of impact processes and by experiments. Laboratory impacts at 6 km/s into water produce an average initial temperature of about 5000 K and an average initial pressure of about 10^6 bar (Lyzenda et al., 1982). Klumov et al. (2005) obtained $T_0 = 10{,}000$ K and $P_0 = 10{,}000$ bars, respectively, for an impact into copper at 10 km/s. Pressure varies within the fireball, however, and a significant portion has a much lower initial pressure. Moreover, one of the main uncertainties of our numerical simulations is caused by lack of knowledge of the equations of state of meteoroids and the regolith of Mercury. We use in our calculations $T_0 = 10{,}000$ K and $P_0 = 10{,}000$ bars. The accuracy of estimation of initial temperature is about 30% because this value may be estimated during impact experiments and observations of impact events in the Solar System. However, the initial pressure cannot be estimated by this way, and the accuracy of its value is about a factor of 3.

The impact-induced cloud is assumed to cool reversibly and adiabatically so that

$$T_0/T = (P_0/P)^{(\gamma-1)/\gamma}, \tag{3}$$

where T and P are the temperature and pressure in the fireball during its expansion. The ratio of specific heats γ is taken to be 1.2 which is typical for mixtures of hot diatomic and triatomic molecules. Pressure rapidly decreases with decreasing temperature and is equal to 400, 40, and 0.6 bar at 6000,

Please cite this article in press as: A.A. Berezhnoy, B.A. Klumov, Impacts as sources of the exosphere on Mercury, Icarus (2008), doi:10.1016/j.icarus.2008.01.005

4000, and 2000 K, respectively. Changing the fireball chemical composition and temperature changes γ. The uncertainty in the quenching pressure attributable to our assumption of constant γ value during impact-induced cloud expansion estimation is about a factor of 10. For example, increasing γ from 1.2 to 1.3 increases the quenching pressure by a factor of 10.

2.2. Elemental composition of the fireball and recapture of ejected material

The chemical composition of the impact-induced cloud depends in part on its initial elemental composition, which is determined by the elemental composition of the surface of Mercury and of the impactors, and by the impactor–target mass ratio. The elemental composition of the mercurian regolith is taken to be a mixture of 90% plagioclase and 10% pyroxene in volume as proposed by Cremonese et al. (2005). The elemental composition of impacting meteoroids is taken to be that of CI chondrites (Lodders and Fegley, 1998).

We use in our calculations a target–impactor mass ratio equal to 30:1 which corresponds to an impact velocity of 40 km/s. In this case the impactors are the main source of volatile elements such as N, C, and H in the cloud while the content of non-volatile elements is determined mainly by the regolith elemental composition. Namely, the relative abundances of main elements in the cloud by number of atoms are the following: O—60.64, Si—18.71, Al—10.16, Ca—3.94, Na—3.36, H—1.33, Mg—1.1, Fe—0.37, C—0.19, S—0.11, K—0.068, N—0.015, and Ti—0.005. However, preferred vaporization of volatile elements from the planet can lead to depletion of refractory elements in the impact-induced cloud.

After a meteoroid impact, Mercury recaptures some of the mass ejected. To estimate this mass we use the technique of Berezhnoi and Klumov (1998). As numerical calculations show, the velocity distribution $V(r)$ along the radius r in the impact vapor cloud is close to linear: $V(r) \sim V_{\max} r/R_{\max}$, where $V_{\max}$ is the expansion velocity of the hot cloud and $R_{\max}$ is the radius of the cloud. The expansion velocity of the hot cloud is estimated as $V_{\max} \approx V_{\rm i}(M_{\rm i}/M_{\rm v})^{0.5}$. The spatial mass distribution function in the fireball is assumed to be the same as for the case of a point explosion at $\gamma = 1.2$ (Zel'dovich and Raizer, 1966). It is assumed that the impactor and target material are well mixed.

Based on the spatial distribution function and velocity distribution in the fireball we can estimate the mass fraction of the cloud captured by Mercury. Namely, the mass fraction of impact-formed vapor captured by Mercury decreases slightly with increasing impact velocity, from 0.1 at 20 km/s to 0.07 at 60 km/s impacts. In our calculations, the fraction of the vapor cloud retained on the planet decreases with increasing impact velocity more slowly than that in the calculations of (Moses et al., 1999). This difference arises because we assume $M_{\rm v} \sim (V_{\rm i})^{2-\nu}$ based on formula (2) while Moses et al. assume that the masses of impactor and target material in the impact-induced cloud are equal and independent of impact velocity.

2.3. Quenching of chemical reactions

At the beginning of impact-induced cloud expansion, the chemical composition can maintain thermodynamical equilibrium because collisions occur frequently and chemical reactions are fast. The equilibrium chemical composition of the cloud at any moment depends on its temperature and pressure. We describe next the use of quenching theory in estimating the chemical composition of the cloud as it cooled to the point where chemical reactions effectively stopped. It is assumed that chemical reactions end or quench, and that the chemical composition is fixed when two quantities, the chemical and hydrodynamic time scales, become comparable. Let us estimate the chemical and hydrodynamic time scales.

The hydrodynamic time scale can be estimated as R/V, where R is the radius of the cloud at the time of quenching, and V is the velocity of the cloud expansion. Based on Eq. (3) at accepted $\gamma = 1.2$, $T_0 = 10{,}000$ K, and $T_{\rm q} \sim 2500$ K as it is estimated below, the radius of the cloud at the time of quenching is about 10 radii of the impactor. According to numerical modeling of impact events (for example, Klumov et al., 2005) the expansion velocity of an impact-produced cloud is of the order of the sound speed. For this reason the cloud expansion speed is taken to be the speed of sound in the hot vapor, about 1 km/s. About 75% of the meteoroid mass flux is in the size range of 10^{-3}–10^{-2} m; meteoroids in the size range 10^{-2}–10^{-1} m account for the rest of the mass flux (Cremonese et al., 2005). Thus, the hydrodynamic time scale for majority of meteoroid impacts can be estimated as 10^{-7}–10^{-5} s.

The chemical time scale for destruction of a compound A in a reaction of the form $A + B = C$ can be approximated as $[A]/|d[A]/dt|$ or $(k[B])^{-1}$, where $[A]$ and $[B]$ is the equilibrium abundance of compounds A and B, respectively, which depends on temperature, pressure, and elemental composition, and $k(T)$ is the rate constant, which is expressed in the form of $k_0 e^{-T_{\rm a}/T}$, where k_0 is the pre-exponential factor, T is the temperature of the species, and $T_{\rm a}$ is the so-called activation temperature. To estimate the chemical time scale we use our calculated equilibrium chemical composition and rate constants taken from the NIST chemical kinetics database extrapolated to higher temperatures. To determine the rates of formation and destruction of a given compound we choose the fastest reactions in which this compound participates.

The hydrodynamic time scale increases linearly with the radius of the cloud. The time scales of chemical reactions increase even more rapidly with fireball expansion due to decreasing concentrations of reagents and the exponential decrease of most reaction rates with decreasing temperature. The quenching parameters are determined by the initial parameters of the fireball expansion, the hydrodynamic and chemical time scales.

Comparisons of reaction rates reveal that the main processes determining H_2O, OH, SH, S, SO, SO_2 contents are the reactions $H + H_2O = H_2 + OH$, $H_2 + OH = H_2O + H$, $O + SH = SO + H$, $S + H_2 = SH + H$, $H + SO = S + OH$, $SO_2 + M = SO + O + M$, respectively. We find that reactions in which H-, O-, and S-containing species participate typically quench at $T_{\rm q} \sim 3500$ K and $P_{\rm q} \sim 30$ bars.

Please cite this article in press as: A.A. Berezhnoy, B.A. Klumov, Impacts as sources of the exosphere on Mercury, Icarus (2008), doi:10.1016/j.icarus.2008.01.005

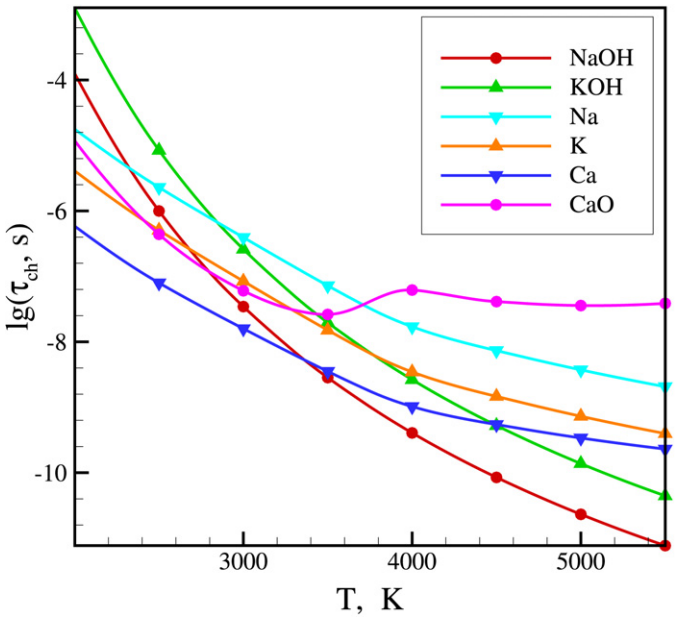

Fig. 1. Time scale of several chemical reactions involving Na-, K-, Ca-containing species in the impact-induced cloud starting its adiabatical cooling at $T_0 = 10{,}000$ K and $P_0 = 1000$ bars. Curves NaOH, KOH, Na, K, Ca, CaO represent the following chemical reactions: NaOH + M = NaO + H + M, KOH + M = KO + H + M, Na + O_2 + M = NaO_2 + M, K + O_2 + M = KO_2 + M, Ca + O_2 = CaO + O, CaO + H_2O = $Ca(OH)_2$, respectively.

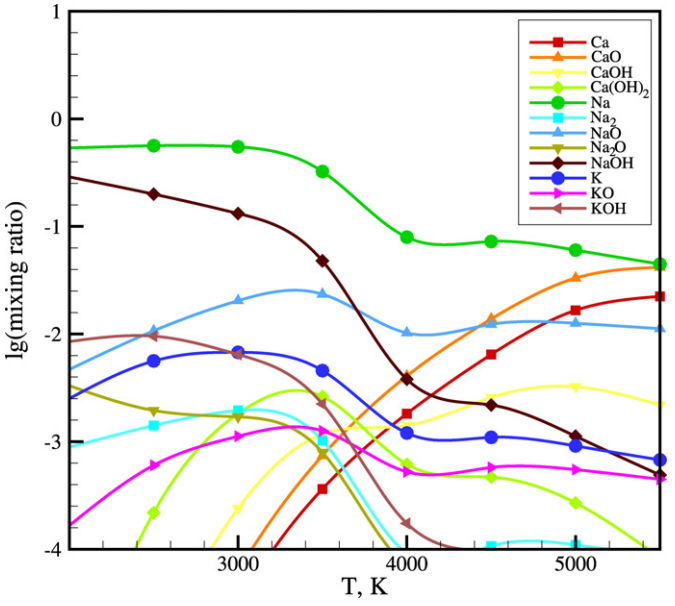

Fig. 2. Equilibrium fraction of gas-phase Na-, K-, Ca-containing species versus temperature during cloud cooling. Initial temperature is 10,000 K, initial pressure is 10,000 bar, $\gamma = 1.2$. Ratio of matter of planetary and CI meteorite origin is taken to be 30:1.

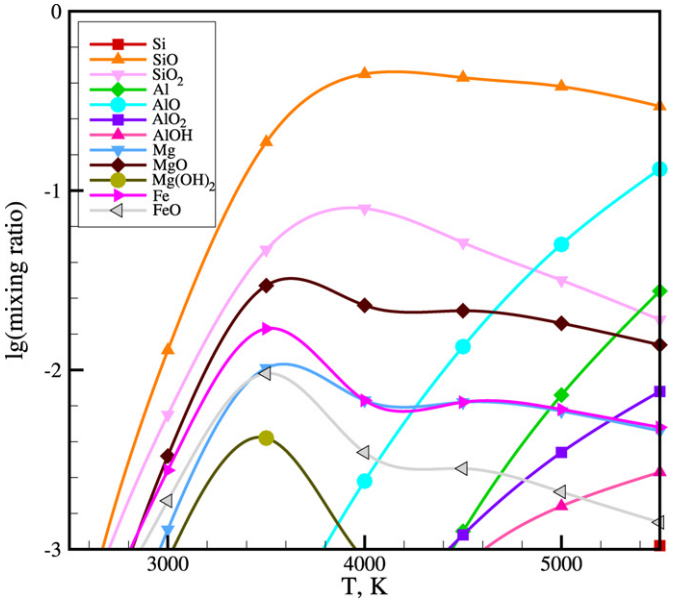

Fig. 3. Equilibrium fraction of gas-phase Si-, Fe-, Mg-, Al-containing species versus temperature during cloud cooling. Initial temperature is 10,000 K, initial pressure is 10,000 bar, $\gamma = 1.2$. Ratio of matter of planetary and CI meteorite origin is taken to be 30:1.

The main and fastest reactions in which Na-, K-, Ca-containing species participate are NaOH + M = Na + OH + M, Na + O_2 + M = NaO_2 + M, KOH + M = KO + H + M, K + O_2 + M = KO_2 + M, $Ca(OH)_2$ = CaOH + OH, $Ca(OH)_2$ = CaO + H_2O, CaO + H_2O = $Ca(OH)_2$, CaOH + OH = $Ca(OH)_2$. The time scales of these reactions are comparable with hydrodynamic time scale (10^{-7}–10^{-5} s) for meteoroid impacts for which $T_q \sim 2500$ K and $P_q \sim 3$ bars (see Fig. 1). Reactions in which Mg-, Al-, Fe-containing species participate also have similar quenching temperatures and pressures.

2.4. *Delivery of species to the exosphere by impacts*

Having chosen the initial elemental composition, temperature, and pressure of the impact-induced cloud, we followed the evolution of its equilibrium chemical composition using a thermochemical code. Abundances of species were calculated by standard methods of Gibbs free energy minimization. Our code allows calculations of equilibrium compositions for up to 102 species made from up to 15 elements. Thermodynamic properties of the considered species were taken mainly from the database of Gurvich et al. (1989). This database comprises data for 1832 species including ions, atoms, and molecules.

At the high temperatures and pressures prevailing immediately after an impact, atoms are more abundant than molecules in the cloud. As the cloud expands and cools, complex species form. At quenching, the major components of an impact-induced cloud are Na, NaOH, and O_2. The elements K, Al, Mg, Fe are present in the gas phase mainly as KOH, K, AlO, Mg, MgOH, Fe (see Figs. 2 and 3). Even at 6500 K Ti is present not as atoms but as molecules of TiO(g), at lower temperatures, TiO_2 is the main Ti-containing compound. For temperatures lower than 3500 K, Ca is present mainly in the solid state, the main gas-phase Ca-containing compound is $Ca(OH)_2$(g). Consistent with these findings, Killen et al. (2005) reported the presence of very hot Ca atoms in the exosphere and attributed them to the photodissociation of CaO released to the exosphere by meteoritic impacts.

The abundances of gas phase species of refractory elements rapidly decrease with decreasing temperature at 3000–5000 K

Please cite this article in press as: A.A. Berezhnoy, B.A. Klumov, Impacts as sources of the exosphere on Mercury, Icarus (2008), doi:10.1016/j.icarus.2008.01.005

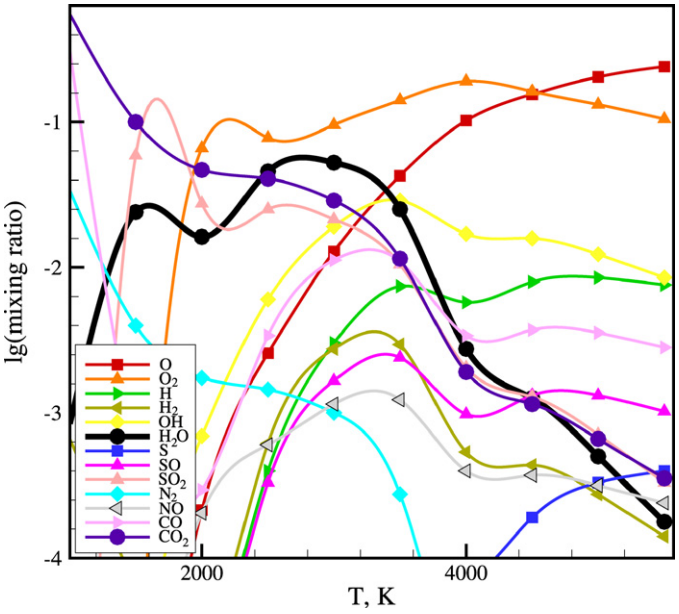

Fig. 4. Equilibrium fraction of gas-phase H-, O-, S-, N-containing species versus temperature during cloud cooling. Initial temperature is 10,000 K, initial pressure is 10,000 bar, $\gamma = 1.2$. Ratio of matter of planetary and CI meteorite origin is taken to be 30:1.

due to the formation of solid phases. However, species containing Na or K do not condense even at 2000 K. In general, condensation enriches volatile elements and depletes refractory elements in the gas phase.

Molecular species have not yet been observed in Mercury's exosphere. For this reason we focus on the factors that control the vapor-phase concentrations of metal atoms. At quenching (2500 K and 3 bars), the fractions of Na(atoms)/Na(total) and K(atoms)/K(total) in the fireball are estimated as 0.7 and 0.4, respectively (see Fig. 2). The corresponding fractions are much lower for more refractory Mg, Ca, and Al because these elements form molecules or condense to form solids (in equilibrium MgO, CaO, and Al_2O_3, respectively). We do not consider condensation of minerals because minerals are not included in thermochemical code used. Chemical reactions and condensation in the cloud significantly reduce the fraction of metallic atoms delivered to Mercury's exosphere directly by meteoroid impacts (see Section 2.5).

For a wide range of T_q and P_q and especially when impact velocities are low, NaOH, water, and hydroxyl are the main components among H-containing species in the cloud (see Figs. 2 and 4). Thus, meteoroid impacts may be considered as a significant potential source of water molecules on Mercury if condensation does take place. Hydroxyl molecules can react with the minerals on the surface and form hydrosilicates.

Sulfur is in the gas phase when the chemical composition quenches because the formation of solid FeS is kinetically prohibited in the fireball (Berezhnoy et al., 2003). The main S-containing species at quenching are SO_2 and SO while the main C-containing species are CO_2 and CO (see Fig. 4). The main N-containing species are N_2 and NO while main O-containing species are NaOH and O_2 (see Figs. 2 and 4).

2.5. Limitations of quenching theory

In estimating the quenching parameters of the impact-induced cloud, we considered only gas-phase reactions. In reality, appreciable concentrations of condensed phases are probably present and may influence the course of chemical reactions. For example, dust grains with a size of about 10^{-7} m were effectively produced for about 10^{-3} s in the fireballs formed after the Comet Shoemaker–Levy 9–Jupiter collision (Friedson, 1998). Dust is a very effective catalyst of chemical reactions at low temperatures and for this reason our estimates of P_q and T_q may be too high.

We make several other assumptions in modeling the chemical composition of the impact-induced cloud. The parameters of impacts such as the initial temperature and pressure, and target/impactor mass ratio in the cloud are assumed to be independent of impactor size and velocity, and of the elemental composition and density of both the impactors and the regolith. In our modeling calculations we assume that the cloud can be characterized by a single temperature and pressure. In reality the impact-induced cloud is highly non-uniform. The inner portion of the cloud has a higher temperature and pressure while in the outer parts temperatures may be too low to achieve thermal equilibrium. Different reactions have different rate constants and therefore different quenching parameters. Increasing the size of the impactors and the initial pressure lead to decreases of the quenching temperature and pressure.

Thus, the assumption of the same quenching parameters for all impacting meteoroids, all reactions and all parts of the cloud is a significant simplification of the problem. However, as we will show later, the exact estimation of the chemical composition of the cloud at the time of quenching is not the final step of changing of the chemical composition of the cloud because the chemical composition of impact-produced species in the exosphere of Mercury is determined by photolysis of species originally delivered to the exosphere by impacts. Due to limitations of quenching theory the accuracy of estimated fractions of minor compounds in the impact-induced cloud at the time of quenching is about a factor of 3. This value is estimated better for major compounds because for these compounds some uncertainties like dust formation, and errors of quenching parameters are not as significant as for minor compounds.

3. Photolysis of molecules in the exosphere

3.1. Ballistic flight times

Let us estimate the impact of photolysis processes on the chemical composition of impact-produced species. Photolysis of metal oxides and hydroxides by solar photons leads to the formation of atoms of metals, hydrogen atoms, and oxygen atoms. The fraction of molecules destroyed during ballistic flight may be estimated by comparing ballistic flight times and photolysis lifetimes.

The ballistic flight time t can be estimated as $2 \times V_{th}(z)/g$, where $V_{th}(z)$ is z-component of the thermal velocity of molecules, and $g = 3.7$ m/s^2 is the surface gravity on Mercury. For

Please cite this article in press as: A.A. Berezhnoy, B.A. Klumov, Impacts as sources of the exosphere on Mercury, Icarus (2008), doi:10.1016/j.icarus.2008.01.005

an ideal gas, the thermal velocity of molecules V_{th} is proportional to $(T/M_r)^{0.5}$, where T is the gas temperature; M_r is the molecular mass of the considered species. So ballistic flight times can be estimated as $2 \times (RT/M_r)^{0.5}/g$, where R is the gas constant. The gas temperature is taken as the same as the quenching temperature of chemical reactions. On Mercury, the ballistic flight time of species such as O_2, NaOH, KOH, AlO, MgO, CaO, FeO is about 250–500 s for a gas temperature of about 2000–3000 K and typical molecular masses in the range of 0.03–0.07 kg/mol.

3.2. Method of estimation of photolysis lifetimes of metal oxides

Photolysis lifetimes τ can be determined from solar photo rates J^{-1}. Solar photo rates J in units of s^{-1} of a given compound can be calculated as

$$J = \int_I \sigma(\lambda, T)\phi(\lambda)F(\lambda)\,d\lambda, \tag{4}$$

where σ is the cross section of photolysis, ϕ is photolysis quantum yield, and F is the unattenuated solar flux. Only photons with energies exceeding the binding energy of a molecule cause dissociation. Due to the rapid decrease of the solar photon flux with decreasing wavelength, molecules with high dissociation energies are more stable against solar photolysis than are molecules with low dissociation energies. Typically the photolysis cross section has a maximum at 20–50 nm shorter than the binding energy equivalent wavelength. We assume that the photolysis lifetimes of molecules are proportional to the solar flux at the binding energy equivalent wavelength because the solar flux typically is similar at the binding energy equivalent wavelength and at the wavelength of maximal photolysis cross section.

The photolysis lifetimes of major metal oxides and hydroxides at the orbit of Mercury are unknown. We therefore estimate them based on the photolysis lifetimes and molecular constants of atmospheric diatomic species on the Earth. We assume that photolysis quantum yields and photolysis cross sections are the same for all molecules and independent of wavelength. The unattenuated solar flux, solar photo rates, binding energy equivalents and dissociation energies of atmospheric species were taken from Huebner et al. (1992). The correlation between solar photo rates for quiet Sun and the unattenuated solar flux at λ_{bind} for atmospheric diatomic species such as O_2, Cl_2, CH, HF, C_2, N_2, OH, SO, CN, BrO, HCl, NO is strong ($r^2 = 0.9$), the fit matches available data to within a factor of 10. Differences between predicted and measured solar photo rates are caused by different photolysis cross sections for different molecules. Thus, solar photo rates J at 1 a.u. correlate with the unattenuated solar flux at binding energy equivalent wavelength $F(\lambda_{bind})$ for atmospheric diatomic species as

$$J = 3 \times 10^{-17} \times F(\lambda_{bind}), \tag{5}$$

where F is in photons $cm^{-2}\,s^{-1}\,nm^{-1}$ and λ_{bind} (nm) $= 1240/E$ (eV) is the binding energy equivalent wavelength.

3.3. Photolysis of impact-produced molecules in the exosphere of Mercury

Let us use Eq. (5) for estimation of photolysis lifetimes at 1 a.u. of metal oxides and SiO. However, all atmospheric diatomic species are covalent while metal oxides are ion compounds. It may cause even worse accuracy of used approach than a factor of 10 for estimation of photo rates of metal oxides. The dissociation energies of metal oxides are 2.6 eV for MgO (Bauschlicher et al., 1982), 2.8 eV for KO (Lee et al., 2002), 4.0 eV for CaO (Kalff et al., 1965) and FeO (Murad, 1980), 4.5 eV for SiO (Hildenbrand and Murad, 1969), 5.2 eV for AlO (Reddy et al., 1998), 6.9 eV for TiO (Naulin et al., 1997). Solar photo rates increase with decreasing distance to the Sun r as r^{-2}. From these data and Eq. (5) used for mean heliocentric distance of Mercury (0.39 a.u.) instead of 1 a.u. photolysis lifetimes on Mercury were estimated to be 80, 80, 200, 200, 600, 2000, and 30,000 s for MgO, KO, FeO, CaO, SiO, AlO, TiO, respectively.

Let us note that expression (5) is obtained for atmospheric species with low dipole moments and at 300 K. Metal monoxides have high dipole moments and, respectively, high transition dipole moments. The typical temperature of impact-produced species is about 2500 K while photolysis lifetimes also decrease with increasing temperature of the species. Both factors can lead to a decrease of the photolysis lifetimes. For example, the experimental NaO photolysis lifetime (Self and Plane, 2002) is 50 times shorter than that estimated by Eq. (5).

The probability P of photolysis during a single hop is estimated from:

$$P = 1 - e^{-t/\tau}, \tag{6}$$

where t is the ballistic flight time and τ is the photolysis lifetime. Using Eqs. (5) and (6) we see that the probability of dissociation of MgO, KO, CaO, FeO during its ballistic flight is significantly higher than 90%, and that the probabilities of SiO, AlO, and TiO dissociation are about 60%, 30%, and 5%, respectively. Thus, the chemical composition of an impact-produced exosphere is strongly affected by photochemical processes. Photodissociation leads to the appearance of metal atoms in the exosphere with high velocities comparable to the escape velocity from Mercury of 4.2 km/s. For further elucidation of the behavior of atoms of refractory elements in the Hermean exosphere, laboratory and theoretical measurements of photolysis lifetimes of the oxides considered above are required.

Photolysis lifetimes (Huebner et al., 1992) and ballistic flight times are comparable for main S-containing species in the cloud, SO and SO_2. Thus, a significant fraction of sulfur will be delivered to the exosphere in atomic form. Due to the long photolysis lifetimes of the main N-, C-containing compounds, N_2, NO, CO_2, and CO (Huebner et al., 1992), only about 1% of molecules of these species will be destroyed during its first ballistic flight.

Please cite this article in press as: A.A. Berezhnoy, B.A. Klumov, Impacts as sources of the exosphere on Mercury, Icarus (2008), doi:10.1016/j.icarus.2008.01.005

4. Properties of impact-produced atoms in the exosphere

4.1. Energy of impact-produced atoms in the exosphere

The photolysis lifetimes of NaOH and NaO at 90 km altitude in the Earth's atmosphere and at 300 K are equal to 42 and 11 s, respectively (Self and Plane, 2002). Photolysis lifetimes of NaOH and NaO on Mercury are 7 and 2 s, respectively. These species will be destroyed by solar photons during ballistic flight on Mercury because the photolysis lifetimes are shorter than their ballistic flight times. Thus, meteoritic bombardment leads to formation of two different components of sodium in the exosphere of Mercury, a low-energy component (0.2–0.4 eV) released directly during impact processes, and a high-energy component produced by the photodissociation of NaO and NaOH. The typical excess energy of photolysis products of diatomic molecules is about 1–2 eV, an energy that corresponds to a temperature of 10,000–20,000 K. Thus, the energy of the second component of Na atoms is about 1–2 eV. We now argue that these same two components are represented in the atoms of other elements, in particular K, Ca, Al, Si, and Ti. The typical excess energy of photolysis products slightly increases with increasing dissociation energy of diatomic molecules (Huebner et al., 1992). Thus, the temperatures of Al, Si, Ti atoms formed during the photolysis of their oxides may be higher than those of other elements due to the high values of the AlO, SiO, and TiO dissociation energies.

Short NaOH photolysis lifetime as the main O-, H-containing compound in impact-induced cloud leads to delivery of hot OH molecules to the exosphere. Due to long OH photolysis lifetime, about 10^4 s (Huebner et al., 1992), only about 10% of OH molecules will be destroyed by solar photons during its single hop. Due to the existence of a strong OH resonance line hydroxyl molecules may be detected in the exosphere of Mercury (Killen et al., 1997).

The thermochemical calculations show that metal hydroxides are produced during meteoroid impacts. Let us make the approximation that photolysis lifetimes of metal hydroxides are the same as those of oxides based on similar photolysis lifetimes of NaOH, NaO (Self and Plane, 2002) and H_2O, OH (Huebner et al., 1992). We find that MgOH, KOH, CaOH, and FeOH are almost completely photolyzed during their single ballistic flight while AlOH is more stable against solar photons. The temperatures of atoms formed by a chain of photolysis reactions (for example, $Ca(OH)_2 \rightarrow CaOH \rightarrow CaO$ and $H \rightarrow Ca$ and O) are higher than those formed by photolysis of monoxides because each photolysis process boosts the energy of the photolysis products.

On the night side of the planet photolysis does not occur. Only atoms of several elements such as Na, K, and Fe, which are mainly produced directly by impacts can be detected on the night side. We predict that the energy of the night-side atoms will be about 0.2–0.4 eV.

The search for impact-produced molecules in the Mercury's atmosphere is useful for the determination of the main impact-produced species and for the study of photolysis rates and paths of these species.

4.2. Description of used model for estimation of the composition of impact-produced exosphere

The quantitative theory of Hermean exosphere was already discussed by Morgan and Killen (1997). Let us present Eqs. (1) and (2) of this article in the form $S(X) = (M_v - 1)F_m F_s(X)R_s/A_r(X) + F_m F_i(X)R_{imp}/A_r(X)$, where $S(X)$ is the source rate of considered element X, F_m is meteoroid impact flux, $F_s(X)$ and $F_i(X)$ are fractions of element X in the regolith and impactor, respectively, by mass, $A_r(X)$ is atomic mass of element X, and R_s and R_i are fractions of the cloud of planetary and impactor origin, respectively, captured by Mercury. Transforming to column densities and taking into account the elemental composition of the cloud we obtain

$$[X] = F_v R F(X)\tau_{loss}/A_r(X), \tag{7}$$

where $[X]$ is the zenith column density of element X, F_v is the vapor production rate, $F(X)$ is the fraction of element X by mass in the cloud, R is the fraction of the cloud captured by Mercury, and $\tau_{loss}(X)$ is the typical time scale of loss processes of element X. However, condensation and photolysis were not considered by Morgan and Killen (1997). For this reason we estimate

$$F_x = F_{unc}(X)\big(f_i(X) + f_{ph}(X)\big)\{X\}, \tag{8}$$

where F_x is the fraction of atoms of element X in the gas phase, $\{X\}$ is the fraction of element X in the cloud by number of atoms, $F_{unc}(X)$ is the fraction of uncondensed species of element X in the gas phase, $f_i(X)$ and $f_{ph}(X)$ are ratios between abundance of atoms produced directly during impacts and by photolysis, respectively, and the total abundance of species in the gas phase of the cloud for element X.

We can estimate the concentrations of impact-produced metal atoms in the exosphere of Mercury based on measured Ca concentration. We take the Ca column density as a reference; this approach helps us to avoid estimation of the mass flux of meteoroids on Mercury. We do not take the Na or K column density as reference because atoms of these elements have a low temperature (1500 K) and meteoroid bombardment is a minor mechanism of delivery of Na and K atoms to the exosphere. We consider only impacts as a source of Ca atoms in the exosphere. Normalization of Eqs. (7) and (8) to the measured Ca column density leads to the following equation:

$$[X] = F_{met}(\mathrm{Ca})[\mathrm{Ca}]\{X\}f_x\tau_{loss}(X)F_{unc}(X) \big/ f_{Ca}\tau_{loss}(\mathrm{Ca})\{\mathrm{Ca}\}F_{unc}(\mathrm{Ca}), \tag{9}$$

where $F_{met}(\mathrm{Ca})$ is the fraction of observed Ca atoms delivered to the exosphere by meteoroid bombardment, $[X]$, $[\mathrm{Ca}]$ are the zenith column densities of considered element X and Ca in the exosphere in cm^{-2}, $\{X\}$, $\{\mathrm{Ca}\}$ are the partial concentrations of considered element and Ca in the cloud, $\tau_{loss}(X)$, $\tau_{loss}(\mathrm{Ca})$ are typical lifetimes of considered atoms X and Ca atoms in the exosphere, f_x and f_{Ca} are sum of ratios between abundance of atoms produced directly during impact $f_i(X)$ and by photolysis $f_{ph}(X)$ and total abundance of species in the gas phase of the cloud for X and Ca, respectively, $F_{unc}(X)$ and $F_{unc}(\mathrm{Ca})$ are the

Please cite this article in press as: A.A. Berezhnoy, B.A. Klumov, Impacts as sources of the exosphere on Mercury, Icarus (2008), doi:10.1016/j.icarus.2008.01.005

fractions of uncondensed species of element X and Ca in the gas phase, respectively.

4.3. Content of impact-produced atoms in the exosphere

Let us estimate each component of Eq. (9). The fireball elemental composition ($\{X\}$, $\{\mathrm{Ca}\}$ values) is discussed in Section 2.2 of the paper.

Our thermochemical results (see Fig. 2) and the comparison of ballistic and photolysis lifetimes for CaO show that most impact-associated Ca found in the exosphere of Mercury was not injected directly, but was produced in place by the photodissociation of CaO, CaOH, $Ca(OH)_2$, which formed in the cooling fireball. These results are consistent with the detection of very hot Ca atoms ($T \sim 12{,}000$ K) in the exosphere of Mercury (Killen et al., 2005). While the processes that we have described may account for the very high-energy Ca observed, they may not account for all of the Ca. Ca column densities are known to correlate weakly with solar activity (Killen et al., 2005). Killen and co-workers suggested that ion sputtering of surface materials as the main mechanism of Ca delivery can explain the observed correlation of Ca concentration with solar activity. However, this correlation can also be explained by lower probability of CaO, CaOH, and $Ca(OH)_2$ photodissociation during quiet Sun conditions if the photolysis lifetimes of Ca-containing species are comparable to their ballistic flight times. But our estimation of CaO photolysis lifetime is one order of magnitude shorter than CaO ballistic flight time and it gives indirect evidence that ion sputtering and solar wind are the main sources of Ca in the exosphere.

The increasing intensity of the observed Ca emission line at the poles of Mercury (Bida et al., 2000) cannot be explained by meteoroid bombardment because the meteoroid flux is almost isotropic. Based on the discussion above we use $F_{\mathrm{met}}(\mathrm{Ca})$ value equal to 0.1. Additional observations of Ca during different levels of solar activity, experimental and theoretical estimations of photolysis lifetimes of Ca-containing species are required for better understanding of the role of impacts and ion sputtering as mechanisms of Ca delivery to the exosphere of Mercury.

According to Killen et al. (2005) the Ca tangent column density on Mercury is about 1.3×10^8 cm^{-2}. The Ca zenith column density [Ca] is calculated as 7×10^7 cm^{-2} for the temperature of Ca atoms equal to 12,000 K and the spherical symmetry of Ca atmosphere and taking into account increasing of typical height scale with distance from the planet. The error of this estimation is about 20% because the Ca number density increases near the poles according to Bida et al. (2000).

We assume that atoms and X-containing species of refractory elements are captured by the surface after their first ballistic flight. Then we can take ballistic flight times as lifetimes for atoms of refractory elements. According to Killen et al. (2005) the temperature of Ca atoms is about 12,000 K. We assume that the temperature of Mg, Al, Ti, Si, O atoms is also 12,000 K because they are produced mainly by photolysis of their oxides and hydroxides while the temperature of Na, K, Fe atoms is assumed to be 2500 K because atoms of these elements are produced mainly directly during meteoroid impacts. These values of temperature were used for calculation of ballistic flight times t by the technique described in Section 3.1 of the paper.

If we do not consider the condensation of refractory elements in the cloud we can use $F_{\mathrm{unc}}(X) = 1$ and $F_{\mathrm{unc}}(\mathrm{Ca}) = 1$. The condensation of refractory elements changes the elemental composition in the gas phase and leads to a change of the chemical composition of gas-phase species. The main compounds of the impact-induced cloud at the time of quenching without considering condensation are shown in Table 1.

On the night side of the planet photolysis does not occur and impact-produced atoms are delivered to the exosphere only during impacts, not by photolysis of molecules. To estimate the night-side concentrations of impact-produced atoms we need to use the ratio $f_{\mathrm{x}}(\mathrm{night})$ between abundances of atoms of each considered element X only produced directly by impacts and the total abundance of all X-containing species in the gas phase of the cloud in Eq. (9), and $f_{\mathrm{x}}(\mathrm{night}) = f_{\mathrm{i}}(X)$. Photolysis is an additional source of atoms in the day-side exosphere, $f_{\mathrm{x}}(\mathrm{night}) < f_{\mathrm{x}}(\mathrm{day})$ for all elements, and $f_{\mathrm{x}}(\mathrm{day}) = f_{\mathrm{i}}(X) + f_{\mathrm{ph}}(X)$. However, at quenching parameters Na, K, and Fe are the main components of the cloud among Na-, K-, Fe-containing species, respectively. Accordingly, for these elements $f_{\mathrm{x}}(\mathrm{night}) \approx f_{\mathrm{x}}(\mathrm{day})$ and the expected day-side and night-side concentrations of impact-produced Na, K, and Fe atoms are comparable. The fraction of atoms produced directly by impacts with energies of about 0.2–0.4 eV is estimated based on the quenched chemical composition of the cloud at 2500 K and 3 bars. At quenching parameters (2500 K, 3 bars) $f_{\mathrm{i}}(X)$ is 0.1, 0.02, 0.002, 10^{-8}, and 10^{-9} for Mg, Ca, Al, Si, and Ti, respectively, if condensation takes place. Without considering condensation $f_{\mathrm{i}}(X)$ is 0.9, 0.8, 0.4, 0.2, 0.2, 10^{-4}, 10^{-8}, and 10^{-9} for Na, K, Fe, Mg, Ca, Al, Si, and Ti, respectively. The accuracy of these values is low, about a factor of 10, for Al, Si, and Ti, because equilibrium abundances of gas-phase atoms rapidly decrease with decreasing quenching temperature.

The fraction of molecular species photolyzed during their first ballistic flight can be estimated by comparing ballistic and photolysis lifetimes based on Eq. (6). Photolysis lifetimes of S-, N-, C-containing compounds were taken based on available photolysis lifetimes of SO_2, N_2, CO_2 (Huebner et al., 1992), respectively, because these species are main species of considered elements. Photolysis lifetimes of Ca-, Al-, Mg-, Si-, Ti-containing species were taken as CaO, AlO, MgO, SiO, TiO photolysis lifetimes calculated in Section 3.3 of the paper. This approach is suitable for Mg because MgO is the main Mg-containing compound in the cloud. Al_2O_3, $Ca(OH)_2$, SiO_2, and TiO_2 are main Al-, Ca-, Si-, Ti-containing species and using of AlO, CaO, SiO, and TiO photolysis lifetimes means that Al_2O_3, $Ca(OH)_2$, TiO_2, and SiO_2 photolysis lifetimes are assumed to be equal to AlO, CaO, TiO, and SiO photolysis lifetimes, respectively. NaOH is the main O-, H-containing compound in the cloud if condensation does take place. The NaOH photolysis lifetime is very short (see Section 4.1) and it leads to formation of Na and OH. For this reason photolysis lifetimes of O-, H-containing species are taken to be OH photolysis lifetime (Huebner et al., 1992). Without considering condensation SiO_2 is the main O-containing compound and the photolysis lifetimes

Please cite this article in press as: A.A. Berezhnoy, B.A. Klumov, Impacts as sources of the exosphere on Mercury, Icarus (2008), doi:10.1016/j.icarus.2008.01.005

Table 1
Summary of behavior of the main elements during meteoroid bombardment of Mercury

Element	Main compounds delivered to the exosphere during meteoroid bombardment		Main mechanisms of delivery of atoms to the day-side exosphere during impacts	Day-side concentration of impact-produced atoms, cm^{-2}	
	Without condensation	With condensation		Without condensation	With condensation
Na	Na	Na, NaOH, NaO	Directly by impacts, photolysis	4×10^6	4×10^8
K	K	KOH, K, KO	Directly by impacts, photolysis	6×10^4	6×10^6
Ca	CaO	$Ca(OH)_2$, CaOH, CaO	Photolysis	7×10^6 (reference)	7×10^6 (reference)
Al	Al_2O_3	AlO, AlOH, $Al(OH)_2$	Photolysis	6×10^6	2×10^5
Fe	FeO, Fe	Fe, FeO, $Fe(OH)_2$	Directly by impacts, photolysis	5×10^5	3×10^7
Mg	MgO, Mg	MgO, $Mg(OH)_2$, Mg, MgOH	Photolysis	2×10^6	8×10^7
Si	SiO_2, SiO	SiO_2, SiO	Photolysis	2×10^7	2×10^8
Ti	TiO_2	TiO_2	Photolysis	4×10^2	4×10^4
O	SiO_2, SiO	NaOH, O_2	Photolysis	2×10^8	6×10^8
H	CaOH, $Ca(OH)_2$	NaOH, H_2O	Photolysis	2×10^6	2×10^8
S	SO_2	SO_2, SO	Photolysis	3×10^6	8×10^6
N	NO, N_2	N_2, NO	Photolysis	4×10^3	4×10^5
C	CO_2	CO_2, CO	Photolysis	10^5	10^7

of O-containing species are taken to be the same as the SiO photolysis lifetime. Based on the photolysis lifetimes described above we estimate the f_x(day) value as 1, 1, 0.3, 0.6, and 0.05 for Mg, Ca, Al, Si, and Ti, respectively. Thus the night-side concentrations of impact-produced atoms of Mg, Ca, Al, Si, and Ti are much lower than those at the day side of the planet because $f_x(\text{night}) \ll f_x(\text{day})$ for these elements.

Based on our modeling calculations described above, we estimate the impact-produced Na, K, Si, Al, Mg, Fe, Ti column densities (see Table 1). We use Eq. (9) for estimation of column densities of atoms of volatile elements such as O, H, S, C, and N also. In this case $F_{\text{unc}}(X) = 1$ for $X = $ H, S, C, N and $F_{\text{unc}}(\text{O}) < 1$ because metal oxides can condense and form solids. Let us note that volatile species such as S, CO, CO_2, H_2O, OH, SO, SO_2, N_2, NO, and O_2 are not captured by the surface after their ballistic flight time. For example, sulfur atoms may migrate on the surface and form polar caps as discussed by Sprague et al. (1995). Loss of atoms of volatile elements is controlled by slow processes such as photolysis (typical photolysis lifetimes are about 10^5 s for CO, CO_2, N_2, and NO), and photoionization (typical photoionization lifetimes are 10^5–10^6 s for O and S). Let us assume that the typical loss time τ_{loss} is equal to S photoionization lifetime, OH, N_2, and CO photolysis lifetimes (Huebner et al., 1992) for S, H, O, N, and C, respectively. The values of column densities of O, S, N, C presented in Table 1 are very preliminary because we do not know the mechanisms of interaction of atoms of volatile elements with the surface of the planet.

The condensation of solid phases can significantly reduce the content of metal-containing species in the gas phase in the fireball. To take condensation into account we need to estimate fractions $F_{\text{unc}}(X)$ and $F_{\text{unc}}(\text{Ca})$. Let us assume that fractions of uncondensed species of each element correspond to the equilibrium chemical composition of the fireball at quenching parameters of chemical reactions (2500 K and 3 bars). For our quenching parameters, we expect $F_{\text{unc}}(X = \text{Na, K, Fe, Mg, Ti}) > F_{\text{unc}}(\text{Ca})$, and $F_{\text{unc}}(X = \text{Si}) \approx F_{\text{unc}}(\text{Ca})$, but for Al $F_{\text{unc}}(X = \text{Al}) < F_{\text{unc}}(\text{Ca})$. Our equilibrium condensation model gives higher values of exospheric content than our model without condensation for all considered elements except Al because Ca is condensed at higher temperatures than all these elements except Al.

We think that the real impact-produced concentrations of the main elements will be intermediate between those modeled without condensation and those modeled with equilibrium condensation. The reason is that condensation is highly disequilibrium process at such short hydrodynamic time scales. For example, during impact experiments the relative volatility of Al_2O_3 and CaO is higher than that of the usually more volatile MgO (Gerasimov et al., 1998).

4.4. Comparison of our models with observations

Sodium atoms mainly are delivered to the exosphere of the planet by photon simulated and thermal desorption (Yakshinskiy and Madey, 2000). On Mercury the Na zenith column density is 3×10^{11} cm^{-2} and the K zenith column density is about 10^9 cm^{-2} (Leblanc et al., 2007). The observed temperature of Na atoms in the exosphere is too low to explain on the basis of impacts as the main source of sodium. In particular, Killen et al. (1999) estimate the exospheric abundance of hot Na atoms with a temperature of about 6500 K—a value two times higher than typical for meteoroid impacts—to be less than 1% from the total Na content or 3×10^9 cm^{-2}. The fraction of Na atoms with a temperature of 2500 K which is typical for meteoroid impacts is still unknown, but higher than that with temperatures of about 6500 K. Our model without condensation gives the column density of impact-produced Na atoms as 5×10^6 cm^{-2}. This value is too low to be checked by current techniques. At assumed parameters of equilibrium condensation (2500 K, 3 bars) $F_{\text{unc}}(\text{Na}) = 1$ while $F_{\text{unc}}(\text{Ca}) \ll 1$. The fraction of Ca-containing species $F_{\text{unc}}(\text{Ca})$ in the gas phase is 0.2, 0.01, and 3×10^{-4} at equilibrium condensation temperature of 4500, 3500, and 2500 K, respectively. Due to the rapid decrease of $F_{\text{unc}}(\text{Ca})$ with decreasing temperature the column density of impact-produced Na atoms increases with decreasing tempera-

Please cite this article in press as: A.A. Berezhnoy, B.A. Klumov, Impacts as sources of the exosphere on Mercury, Icarus (2008), doi:10.1016/j.icarus.2008.01.005

ture [see Eq. (9)]. For this reason, our model with equilibrium condensation at 2500 K gives very high values of the concentration of impact-produced Na atoms (2×10^{10} cm^{-2}), which contradicts the observations of the sodium tail of Mercury confirming that ion sputtering is main mechanism of delivery of energetic Na atoms to the tail (Potter and Killen, 2008). The equilibrium condensation in the impact-induced cloud at temperatures lower than 3000 K gives too high an amount of hot Na atoms in the exosphere. For this reason during calculations of column densities of impact-produced atoms in the exosphere we assume that the temperature and pressure of equilibrium condensation is 3500 K and 20 bars, respectively (see Table 1). The accuracy of the calculated column densities is about a factor of 3 because equilibrium fractions of uncondensed gas-phase species rapidly decrease with decreasing condensation temperature. Future observational data will place stronger constraints on the role of condensation of main elements during meteoroid impacts.

Let us compare our predictions of abundances of impact-produced exospheric atoms with the model of Morgan and Killen (1997). Based on the estimated meteoroid mass flux on Mercury, Morgan and Killen (1997) obtain column densities of 5×10^9 cm^{-2} for Al, 7×10^{10} cm^{-2} for Mg, 3×10^9 cm^{-2} for Ca, 2×10^{10} cm^{-2} for Si, and 7×10^8 cm^{-2} for Fe. These values are higher by 1–3 orders of the magnitude than those estimated by our models. For example, with use of intermediate elemental composition of the surface of the planet (Goettel, 1988) the model of Morgan and Killen predicts a Ca content that is about 20 times higher than the observed value. As we use the measured Ca content as a reference, our estimated abundances of impact-produced atoms of refractory elements are much lower than those predicted by Morgan and Killen (1997). Differences between our models and the model of Morgan and Killen can be explained mainly by the fact that they use another technique and do not consider the condensation of solid phases in the fireball. In any case, we would argue that the condensation of solid phases must reduce the content of atoms in the gas phase.

4.5. Ionization of atoms in the exosphere

We have not considered the ionization of atoms by solar photons, but this process can significantly reduce the concentrations of neutral atoms in the exosphere if the photoionization lifetimes of atoms are much shorter than their ballistic flight times. Let us estimate the ionization lifetimes of elements considered. Using ionization rates and ionization energies for atmospheric atoms such as C, N, O, Na, F, S, Cl, Ar, K, Xe (Huebner et al., 1992) we find that the correlation between ionization rates J_i at 1 a.u. and ionization energies E_i for these atoms is strong ($r^2 = 0.9$). Values of photoionization rates predicted with this correlation are though to be good within a factor of 2:

$$\mathrm{Log}\, J_i\ (\mathrm{s}^{-1}) = -0.18 \times E_i\ (\mathrm{eV}) - 4. \quad (10)$$

Using Eq. (10) and the ionization energies of atoms at http://physics.nist.gov/PhysRefData/ we can estimate ionization lifetimes at the heliocentric distance of Mercury as 20,000–40,000 s for other atoms like Ca, Al, Mg, Ti, Fe, and Si. Ionization lifetimes of Na and K are equal to 10,000 and 7000 s, respectively (Huebner et al., 1992). Thus, only several percent of the atoms under consideration can be ionized during a ballistic flight lasting about 250–500 s. However, using much shorter ionization lifetime of Ca atoms equal to 2300 s Killen et al. (2005) obtain higher fraction of ionized Ca atoms in comparison with our results.

4.6. Solar wind as a source of Ca exosphere

Noting the similarity between Ca/O ratio of about 0.002 in the Mercury's exosphere and in the solar wind, Koehn and Sprague (2007) proposed that solar wind, rather than meteoroids or the planet itself, is the main source of calcium in Mercury's exosphere. If so, then the abundances and temperatures expected for main elements in the exosphere will be quite different from those calculated in our modeling of impacts. According to our model without condensation, the Ca/O ratios are similar for the exosphere and the regolith surface, which is estimated as 0.07 on Mercury (Cremonese et al., 2005). This value is significantly higher than the observed Ca/O ratio in the exosphere and in the solar wind. Condensation of dust grains in an impact-induced cloud can significantly reduce the content of refractory elements in the exosphere. Release of hot O atoms during photodissociation of O-containing species decreases Ca/O ratio in the exosphere also. The Ca/O ratio is about 0.01 at temperature of condensations of refractory elements of about 3500 K. Thus, both our models give higher Ca/O ratio than observed value and meteoroid bombardment is only minor source of atomic oxygen in the exosphere of Mercury.

5. Conclusions

The behavior of main elements released during/after meteoroid bombardment of Mercury is summarized in Table 1. The main compounds of impact-produced cloud at the quenching point are presented. Column densities of impact-produced atoms of main elements normalized to the Ca column density were calculated without considering condensation of dust grains in the cloud and for the assumption of equilibrium condensation at 3500 K and 20 bars. The real column densities probably lie between these two values because condensation is a very slow process and it cannot occur at equilibrium conditions for the very short times typical of expansion of the cloud. Values of column densities of impact-produced atoms are valid only on sunlit side of Mercury, since no photodissociation takes place on the night side.

Based on quenching theory, we have estimated the chemical composition of gas-phase species released to the Hermean atmosphere during meteoroid impacts. Chemical reactions in the fireball effectively cease at the point when Ca, Mg, Al, Si, and Ti have formed oxides. Hydroxides of Na, K, Ca, and Mg are also produced during collisions between meteoroids and Mercury. Once formed, however, a significant fraction of these oxides and hydroxides is destroyed by solar photons because

Please cite this article in press as: A.A. Berezhnoy, B.A. Klumov, Impacts as sources of the exosphere on Mercury, Icarus (2008), doi:10.1016/j.icarus.2008.01.005

for these compounds ballistic flight times are longer than photolysis lifetimes. The photolysis of MgO, KO, FeO, CaO occurs on average at a distance of about 300 km from the place of meteoroid impact. Accordingly, measurements of abundances of Mg, K, Fe, Ca atoms—atoms that come primarily from vaporized regolithic material—with high spatial resolution may be useful for mapping of the abundances of these elements at the surface. Our results predict that the content of impact-produced Ca and Mg atoms in the planetary exosphere is almost independent of solar activity because CaO and MgO photolysis lifetimes are significantly shorter than CaO and MgO ballistic flight times for all levels of the solar activity. Al and Ti content in the exosphere may be higher during periods of active Sun and at perihelion because photolysis lifetimes are longer than the ballistic flight times for AlO and TiO. A weak dependence of exospheric content of impact-produced atoms on the distance of the planet from the Sun may also reflect changes of meteoroid impact flux with heliocentric distance.

Based on the model of chemistry of impact-induced cloud without condensation of solid phases, the content of impact-produced atoms of Na, K, Ca, Fe, Mg, Si in the exosphere will be proportional to the content of these elements at the surface of the planet while Al and Ti are depleted in the exosphere due to the long photolysis lifetimes of their oxides. However, condensation of dust grains does take place and it leads to significant decreases in the content of non-volatile elements in the gas phase such as Al, Ca, Fe, Mg, Ti, and Si.

Meteoroid bombardment leads to the appearance of hot metal atoms ($E \sim 0.2$–0.4 eV) produced directly by impacts and of very hot atoms ($E \sim 1$–2 eV) formed during photodissociation of metal oxides and hydroxides. Atoms of Na, K, and Fe are produced mainly directly by impact while atoms of Ca, Al, Mg, Si, and Ti are delivered to the exosphere by photolysis of their oxides and hydroxides. It will be possible to measure fractions of hot and very hot atoms by high-resolution spectroscopy by modeling of temperatures and concentrations of metal atoms as function of the altitude based on intensity of atomic lines as function of the altitude.

The chemistry of volatile elements such as H, N, C, and S is also studied. Only sulfur is delivered to the exosphere mainly in atomic form due to the short photolysis lifetime of the main S-containing compound in the impact-induced cloud, SO_2. The main impact-produced H-containing compound in the exosphere is hydroxyl OH formed by photolysis of metal hydroxides.

We have used model calculations to estimate the abundances of impact-produced atoms in the exosphere of Mercury. The main uncertainties in the predicted abundances are caused by the use of the same quenching parameters for all parts of the impact-induced cloud, by the unclear role of the dust grain formation during such impacts, and by limited knowledge of the elemental composition of the surface of Mercury. A comparison of day-side and night-side abundances of refractory elements in the exosphere of Mercury will be useful for understanding the role of meteoroid bombardment in the formation of the exosphere of the planet. Laboratory impact experiments would be useful for a more accurate determination of the quenching parameters.

Acknowledgments

The authors thank G. Michael and G. Herzog for helpful remarks and two anonymous referees for useful suggestions. This research was supported in part by NASA Grant NNGO 5GF82G.

References

Ahrens, T.J., O'Keefe, J.D., 1987. Impact on the Earth, ocean and atmosphere. Int. J. Impact Eng. 5, 13–32.

Bauschlicher Jr., C.W., Lengsfield III, B.H., Liu, B., 1982. The dissociation energy of MgO. J. Chem. Phys. 77, 4084–4087.

Berezhnoi, A.A., Klumov, B.A., 1998. Lunar ice: Can its origin be determined? JETP Lett. 68, 163–167.

Berezhnoy, A.A., Hasebe, N., Hiramoto, T., Klumov, B.A., 2003. Possibility of the presence of S, SO_2, and CO_2 at the poles of the Moon. Publ. Astron. Soc. Jpn. 55, 859–870.

Bida, T., Killen, R.M., Morgan, T.H., 2000. Discovery of Ca in the atmosphere of Mercury. Nature 404, 159–161.

Cintala, M.J., 1992. Impact-induced thermal effects in the lunar and mercurian regoliths. J. Geophys. Res. 97, 947–973.

Cremonese, G., Bruno, M., Mangano, V., Marchi, S., Milillo, A., 2005. Release of neutral sodium atoms from the surface of Mercury induced by meteoroid impacts. Icarus 177, 122–128.

Gerasimov, M.V., Ivanov, B.A., Yakovlev, O.I., Dikov, Yu.P., 1998. Physics and chemistry of impacts. Earth Moon Planets 80, 209–259.

Goettel, K.A., 1988. Present bounds on the bulk composition of Mercury: Implications for planetary formation processes. In: Vilas, F., Chapman, C., Mathews, M. (Eds.), Mercury. University of Arizona Press, Tucson, pp. 613–621.

Gurvich, L.V., and 14 colleagues, 1989. Thermodynamic Properties of Individual Substances, fourth ed. in 5 volumes. Hemisphere Pub Co., New York.

Friedson, A.J., 1998. Formation of refractory grains in Shoemaker–Levy 9 fireballs. Icarus 131, 179–197.

Hildenbrand, D.L., Murad, E., 1969. Dissociation energy and ionization potential of silicon monoxide. J. Chem. Phys. 51, 807–811.

Huebner, W.F., Keady, J.J., Lyon, S.P., 1992. Solar photo rates for planetary atmospheres and atmospheric pollutants. Astrophys. Space Sci. 195, 1–289. 291–294.

Kalff, P.J., Hollander, Tj., Alkemade, C.Th.J., 1965. Flame-photometric determination of the dissociation energies of the alkaline–earth oxides. J. Chem. Phys. 43, 2299–2307.

Killen, R.M., Benkhoff, J., Morgan, T.H., 1997. Mercury's polar caps and the generation of an OH exosphere. Icarus 125, 195–211.

Killen, R.M., Potter, A., Fitzsimmons, A., Morgan, T.H., 1999. Sodium D2 line profiles: Clues to the temperature structure of Mercury's exosphere. Planet. Space Sci. 47, 1449–1458.

Killen, R.M., Bida, Th.A., Morgan, Th.H., 2005. The calcium exosphere of Mercury. Icarus 173, 300–311.

Klumov, B.A., Kim, V.V., Lomonosov, I.V., Sultanov, V.G., Shutov, A.V., Fortov, V.E., 2005. Deep Impact experiment: Possible observable effects. Phys.-Uspekhi 48, 733–743.

Koehn, P.L., Sprague, A.L., 2007. Solar oxygen and calcium in Mercury's exosphere. Planet. Space Sci. 55, 1530–1540.

Leblanc, F., Barbieri, C., Cremonese, G., Verani, S., Cosentino, R., Mendillo, M., Sprague, A., Hunten, D., 2006. Observations of Mercury's exosphere: Spatial distributions and variations of its Na component during August 8, 9 and 10, 2003. Icarus 185, 395–402.

Leblanc, F., and 13 colleagues, 2007. Mercury's exosphere origins and relations to its magnetosphere and surface. Planet. Space Sci. 55, 1069–1092.

Lee, E.P.F., Soldan, P., Wright, T.G., 2002. What is the ground electronic state of KO? J. Chem. Phys. 117, 8241–8247.

Please cite this article in press as: A.A. Berezhnoy, B.A. Klumov, Impacts as sources of the exosphere on Mercury, Icarus (2008), doi:10.1016/j.icarus.2008.01.005

Lodders, K., Fegley, B., 1998. The Planetary Scientist Companion. Oxford Univ. Press, New York.

Lyzenga, G.A., Ahrens, T.J., Nellis, W.J., Mitchell, A.C., 1982. The temperature of shock-compressed water. J. Chem. Phys. 76, 6282–6286.

Mangano, V., Milillo, A., Mura, A., Orsini, S., De Angelis, E., Di Lellis, A.M., Wurz, P., 2007. The contribution of impulsive meteoritic impact vaporization to the hermean exosphere. Planet. Space Sci. 55, 1541–1556.

McClintock, W.E., Lankton, M.R., 2007. The Mercury atmospheric and surface composition spectrometer for the MESSENGER mission. Space Sci. Rev. 131, 481–522.

Morgan, Th., Killen, R.M., 1997. A non-stoichiometric model of the composition of the atmospheres of Mercury and the Moon. Planet. Space Sci. 45, 81–94.

Moses, J.I., Rawlins, K., Zahnle, K., Dones, L., 1999. External sources of water for Mercury's putative ice deposits. Icarus 137, 197–221.

Murad, E., 1980. Thermochemical properties of gaseous FeO and FeOH. J. Chem. Phys. 73, 1381–1385.

Naulin, C., Hedgecock, I.M., Costes, M., 1997. The dissociation energy of TiO determined from a crossed-beam study of the $Ti + NO \rightarrow TiO + N$ reaction. Chem. Phys. Lett. 28, 335–341.

Potter, A.E., 1995. Chemical sputtering could produce sodium vapor and ice on Mercury. Geophys. Res. Lett. 22, 3289–3292.

Potter, A.E., Killen, R.M., 2008. Observations of the sodium tail of Mercury. Icarus 194, 1–12.

Potter, A.E., Morgan, T.H., 1990. Evidence for magnetospheric effects on the sodium atmosphere of Mercury. Science 248, 835–838.

Reddy, R.R., Nazeer Ahammed, Y., Rama Gopal, K., Abdul Azeem, P., Anjaneyulu, S., 1998. RKRV potential energy curves, dissociation energies, gamma-centroids and Franck–Condon factors of YO, CrO, BN, ScO, SiO and AlO molecules. Astrophys. Space Sci. 262, 223–240.

Self, D.E., Plane, J.M.C., 2002. Absolute photolysis cross-sections for $NaHCO_3$, NaOH, NaO, NaO_2 and NaO_3: Implications for sodium chemistry in the upper mesosphere. Phys. Chem. Chem. Phys. 4, 16–23.

Sprague, A.L., Hunten, D.M., Lodders, K., 1995. Sulfur at Mercury, elemental at the poles and sulfides in the regolith. Icarus 118, 211–215.

Zel'dovich, Y.B., Raizer, Y.P., 1966. Physics of Shock Waves and High-Temperature Hydrodynamic Phenomena, vol. 1. Academic Press, New York.

Yakshinskiy, B.V., Madey, T.E., 2000. Desorption induced by electronic transitions of Na from SiO_2: Relevance to tenuous planetary atmospheres. Surf. Sci. 451, 160–165.

Yamakawa, H., Ogawa, H., Kasaba, Y., Hayakawa, H., Mukai, T., Adachi, M., 2004. Current status of BepiColombo/MMO spacecraft design. Adv. Space Res. 33, 2133–2141.

Please cite this article in press as: A.A. Berezhnoy, B.A. Klumov, Impacts as sources of the exosphere on Mercury, Icarus (2008), doi:10.1016/j.icarus.2008.01.005